IKKβ in intestinal mesenchymal cells promotes initiation of colitis–associated cancer

Vasiliki Koliaraki,[1] Manolis Pasparakis,[2] and George Kollias[1,3]

[1]Biomedical Sciences Research Center "Alexander Fleming", 16672 Vari, Greece
[2]Institute for Genetics, University of Cologne, D-50674 Cologne, Germany
[3]Department of Physiology, Medical School, National and Kapodistrian University of Athens, 11527 Athens, Greece

The importance of mesenchymal cells in inflammation and/or neoplastic transformation is well recognized, but their role in the initiation of these processes, particularly in the intestine, remains elusive. Using mouse models of colorectal cancer, we show that IKKβ in intestinal mesenchymal cells (IMCs) is critically involved in colitis–associated, but not spontaneous tumorigenesis. We further demonstrate that IMC-specific IKKβ is involved in the initiation of colitis–associated cancer (CAC), as in its absence mice develop reduced immune cell infiltration, epithelial cell proliferation, and dysplasia at the early stages of the disease. At the molecular level, these effects are associated with decreased early production of proinflammatory and protumorigenic mediators, including IL-6, and reduced STAT3 activation. Ex vivo IKKβ–deficient IMCs show defective responses to innate immune stimuli such as LPS, as shown by decreased NF-κB signaling and reduced expression of important NF-κB target genes. Collectively, our results reveal a hitherto unknown role of mesenchymal IKKβ in driving inflammation and enabling carcinogenesis in the intestine.

Carcinogenesis is a multistep process, during which early neoplastic cells attain hallmark features that enable them to give rise to tumors (Hanahan and Weinberg, 2011). Several other cell types, which constitute the tumor microenviroment, facilitate the acquisition of these hallmarks and, therefore, cancer development (Hanahan and Coussens, 2012). In this context, tumor-promoting inflammation is particularly important as an enabling factor in the acquisition of cancer traits (Mantovani et al., 2008; Grivennikov et al., 2010; Hanahan and Weinberg, 2011). Inflammatory bowel disease is causally linked to colon tumor promotion (Terzić et al., 2010), and the role of both inflammatory and endothelial cells is well appreciated (Hanahan and Coussens, 2012). Intestinal mesenchymal cells (IMCs) are equally important in these processes, as they participate in a complex interactive network with adjacent epithelial and neoplastic cells, as well as other stromal cells, via the supply of cytokines and chemokines, growth and survival factors, proangiogenic molecules, and extracellular matrix remodeling enzymes. This leads either to the maintenance of epithelial homeostasis (Bhowmick et al., 2004; Trimboli et al., 2009; Normand et al., 2011) or, after neoplastic transformation, facilitates the establishment of a proinflammatory and protumorigenic milieu (Kalluri and Zeisberg, 2006; Erez et al., 2010; Hanahan and Coussens, 2012), although the exact molecular mechanisms are yet unknown.

NF-κB is a key regulator of both inflammation and cancer. It is normally found in the cytoplasm bound by the inhibitor IκBα. Various stimuli, such as cytokines (e.g., TNF, IL-1β), TLR ligands, stress signals and UV radiation, activate the IKK complex (IKKα, IKKβ, and NF-κB essential modulator [NEMO]), which in turn phosphorylates IκBα, leading to its degradation and the subsequent release of NF-κB that translocates to the nucleus to facilitate gene transcription (Liu et al., 2012). NF-κB is frequently activated in a variety of tumors and data from animal models highlight its protumorigenic functions (Ben-Neriah and Karin, 2011). This constitutive activation is probably mediated by mutations of its upstream regulators or by inflammatory signals from the microenviroment, as mutations in NF-κB itself are rare (Ben-Neriah and Karin, 2011; DiDonato et al., 2012). IKKβ, a crucial member of the IKK complex, is such an upstream regulator and has been implicated in the protumorigenic role of NF-κB. Especially in colitis-associated carcinogenesis (CAC), intestinal epithelial cell (IEC)–, or myeloid cell–specific deletion reduces tumor burden (Greten et al., 2004).

The NF-κB pathway is also found activated in stromal myofibroblasts surrounding colon adenocarcinomas (Vandoros et al., 2006). Interestingly, a recent study revealed that cancer-associated fibroblasts (CAFs) from skin, cervical, mammary, and pancreatic tumors display a NF-κB–regulated proinflammatory signature that is linked to tumor progression (Erez et al., 2010). However, it is still not determined if such

a mechanism exists also in intestinal tumors and what is its physiological role especially in the early stages of malignancy development before differentiation of resident mesenchymal cells to CAFs. In addition, the microenviromental cues and the stimuli to which mesenchymal cells, such as myofibroblasts of CAFs, respond to acquire their signatures remains largely unknown. Current concepts focus on activation of resident or recruited fibroblasts by biomechanical forces or paracrine signaling, such as IL-1β, TNF, and TGFβ originating from preneoplastic or immune cells (Servais and Erez, 2013). However, direct innate sensing from the mesenchymal stroma should not be excluded. Notably, TLR4 signaling and consequently innate sensing in the stroma is sufficient to cause pathology in CAC but the cell type specificity of this response has remained unknown (Fukata et al., 2009).

In the present study, we explore the IMC-specific role of NF-κB signaling during colitis-associated carcinogenesis using mice with a genetic deletion of *Ikkβ* in IMCs. We show that IMC-specific IKKβ deletion in vivo leads to decreased tumor incidence after exposure to azoxymethane (AOM) and dextran sodium sulfate (DSS) treatment, associated with decreased inflammatory cell infiltration and tissue damage in the early stages of disease development.

RESULTS
Lineage tracing of ColVI–cre^{+} cells in the intestine
To study the role of IKKβ in IMCs, we used mice carrying the ColVIcre transgene, which shows specificity for mesenchymal cells in the joints, skin, heart, and intestine (Armaka et al., 2008). To characterize the exact cell specificity of the ColVIcre mouse in the intestine, we crossed it with the reporter mouse line ROSA^mT/mG (referred to as mT/mG; Muzumdar et al., 2007). In this mouse strain, all cells express the membrane-targeted Tomato sequence. Upon Cre-mediated recombination, this sequence is excised, enabling the expression of membrane eGFP (Fig. 1 A). Samples from the small intestine and colon of these mice showed expression of GFP in the mesenchymal compartment both in homeostatic conditions, as well as in intestinal tumors with a topology similar to that of CAFs (Fig. 1 B).

To further investigate the identity of these cells, we performed FACS analysis of colon and small intestine from ColVIcre-mT/mG mice and verified that they do not express markers of hematopoietic (CD45), erythroid (Ter119), endothelial (CD31), or epithelial origin (E-cadherin). However, they express known markers of mesenchymal cells, such as CD29, CD44, and CD140α, but not CD140β (Fig. 1, C and F). We also performed immunohistochemistry with specific markers for IMCs, such as α smooth muscle actin (α-SMA), vimentin, and Collagen IV (ColIV). GFP⁺ cells expressed these markers; however, we also observed GFP⁻ cells expressing these markers (Fig. 1 D). To quantify these observations, we performed intracellular staining with vimentin and ColIV antibodies and subsequent FACS analysis. This experiment showed that all GFP⁺ cells expressed vimentin and ColIV,

but only ~15% of vimentin⁺ and 22% of ColIV⁺ cells were GFP⁺ in homeostasis (Fig. 1, E–G). Accordingly, around 22% of CD140α⁺ cells were also GFP⁺ (Fig. 1 G).

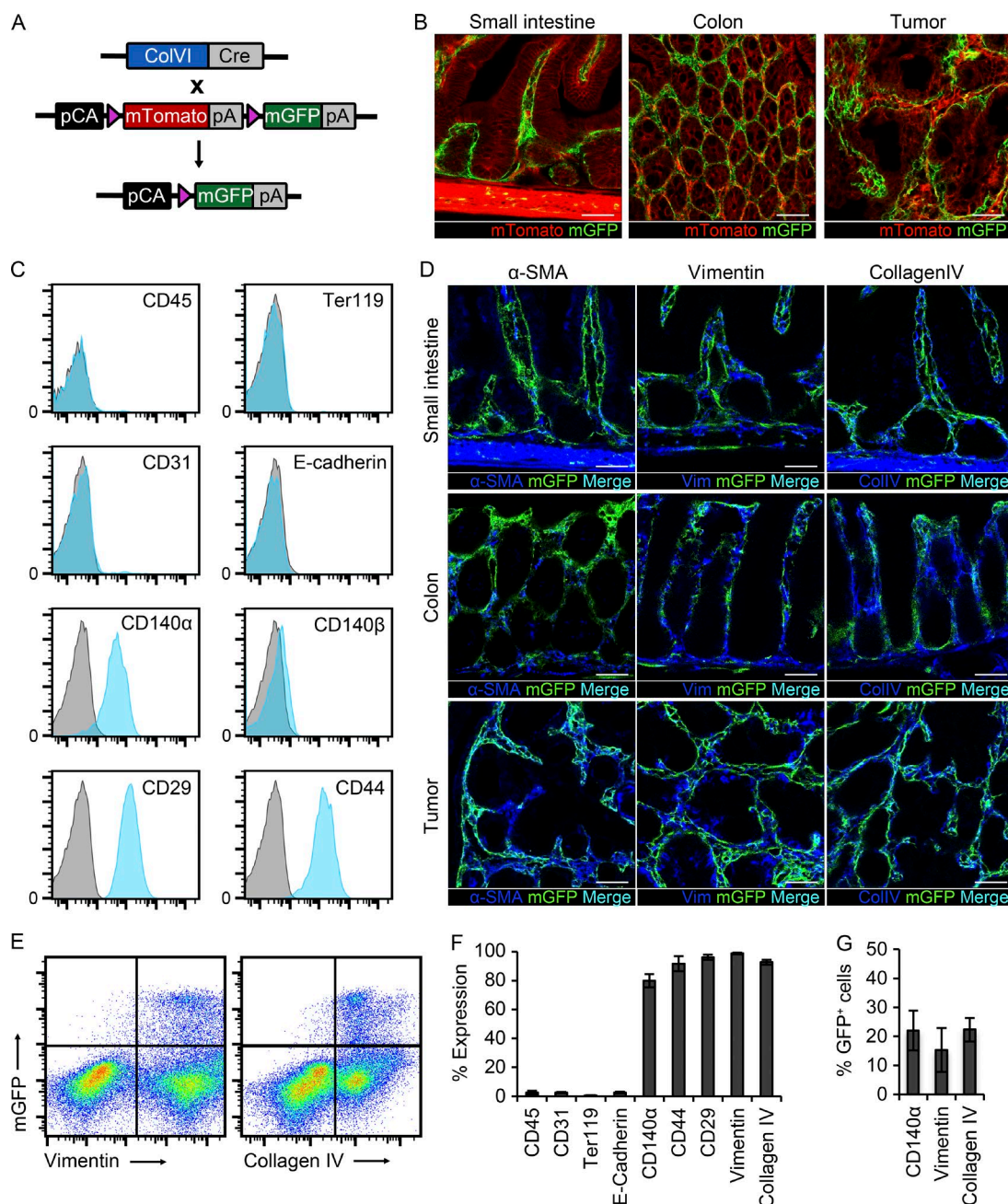From this analysis, it is evident that the ColVIcre mouse targets mainly fibroblast-like cells, which are vimentin⁺ and ColIV⁺ and represent a fraction of the vimentin⁺, ColIV⁺, or CD140α⁺ cells under homeostatic conditions. The ColVIcre mouse does not target smooth muscle cells in the muscle layer, the muscularis mucosa, or the lamina propria, around lymphatic vessels. GFP⁺α-SMA⁺ cells are vimentin⁺ myofibroblasts and pericytes around blood vessels and represent only a small population under homeostatic conditions (Mifflin et al., 2011). It should be noted that in tumors, although ColVIcre-GFP⁺ cells form typical networks and express mesenchymal/CAF markers, they seem to represent only a small fraction of CAFs.

Generation of mice with genetic deletion of IKKβ in IMCs
We then crossed mice carrying the loxP-flanked *Ikkβ* allele (Pasparakis et al., 2002) with ColVIcre mice to achieve IKKβ ablation specifically in mesenchymal cells of the small and large intestine. The resulting ColVIcre-*Ikkβ^F/F* (*Ikkβ^IMCko*) mice were born at the expected Mendelian ratio, were viable and fertile, and did not show any spontaneous intestinal phenotype. We verified the efficiency and specificity of IKKβ deletion in IMCs by Western blot analysis of isolated IMCs (IMCs), IECs, and thioglycolate-elicited peritoneal macrophages (TEPMs) using antibodies against IKKβ and the lineage-specific markers α-smooth muscle actin (α-SMA), E-cadherin, and F4/80, respectively (Fig. 2 A). It should be noted that although few fibroblasts express α-SMA under homeostatic conditions, in culture almost all mesenchymal cells express α-SMA, most likely as a result of the adherence to the plastic surface and the presence of serum in the culture medium. Quantification of these results showed that IKKβ deletion in mesenchymal cell cultures was ~60% (Fig. 2 B). This is in agreement with the percentage of ColVI-GFP⁺ cells from the ColVIcre-mT/mG mouse in cultures, as shown both by FACS analysis and confocal microscopy (Fig. 2, C and D).

IMC-specific genetic deletion of IKKβ protects against inflammation–induced intestinal carcinogenesis
To determine the IMC-specific role of IKKβ in intestinal carcinogenesis, we applied the AOM/DSS model of colitis-associated cancer (CAC). In this model, mice receive a single injection with the carcinogen AOM, followed by three cycles of DSS administration in the drinking water (Fig. 2 E; Neufert et al., 2007). AOM causes mutations and genetic instability in oncogenes in the intestine, whereas DSS, a synthetic, sulfated polysaccharide induces colitis through largely unknown mechanisms that include intestinal barrier disruption and concomitant inflammatory response to commensal microflora by cells in the submucosa. The chronic inflammation caused
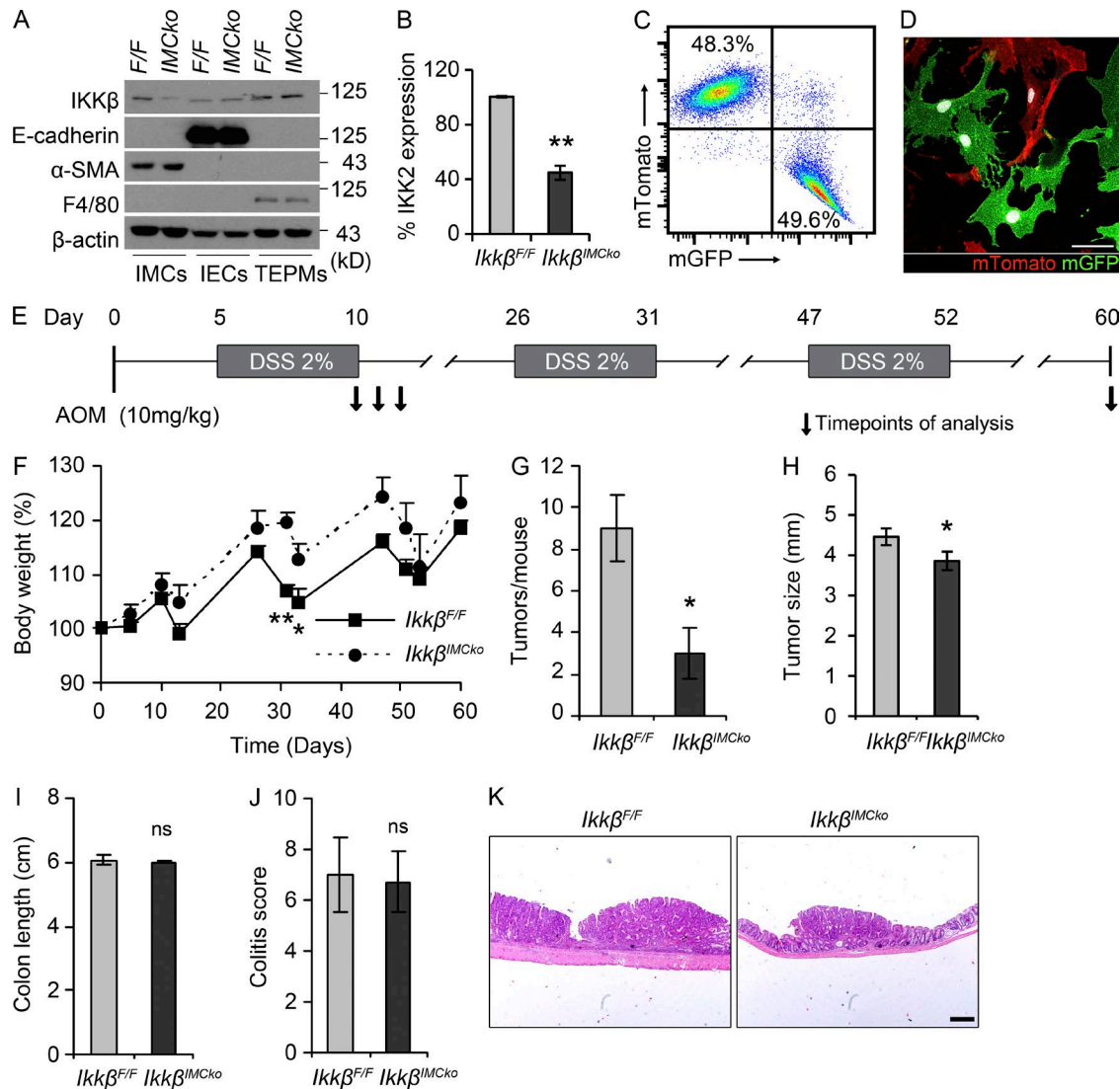
Figure 1. Lineage tracing and characterization of ColVIcre⁺ cells. (A) Schematic representation of crosses between ColVIcre and mT/mG mice. Upon Cre-mediated recombination, the mTomato sequence is excised, allowing the expression of mGFP. Triangles represent loxP sites. (B) Cryosections from small intestine (SI), colon, and colonic tumor samples after AOM/DSS treatment of ColVIcre-mT/mG mice (*n* = 5 mice). Bars, 50 µm. (C) FACS analysis of ColVIcre-GFP expressing cells with markers for hematopoietic (CD45), erythroid (Ter119), endothelial (CD31), epithelial (E-cadherin), and mesenchymal cells (CD140α, CD140β, CD29, and CD44; *n* = 5 mice). (D) Immunohistochemical analysis of samples from small intestine, colon and colonic tumors with antibodies against α-SMA, Vimentin, and CollagenIV (*n* = 5 mice). Bars, 50 µm. (E) FACS analysis of ColVIcre-GFP⁺ cells with intracellular markers Vimentin and Collagen type IV in homeostasis (*n* = 5 mice). (F) Quantification of different marker expression by ColVIcre-GFP⁺ cells in the colon by FACS analysis (*n* = 5 mice). (G) Quantification of the percentage of CD140α⁺, Vimentin⁺, and CollagenIV⁺ cells that are GFP⁺ in ColVIcre-mT/mG mice (*n* = 5 mice). Data are presented as mean ± SE.

by the repeated DSS treatments accelerates both tumor initiation and progression in the colon (Clevers, 2004). *Ikkβ*^*IMCko*^ mice exhibited reduced weight loss during the

first cycles of DSS administration (Fig. 2 F) and a significant lower number of tumors at the end of the protocol in comparison to their littermate controls (Fig. 2 G).
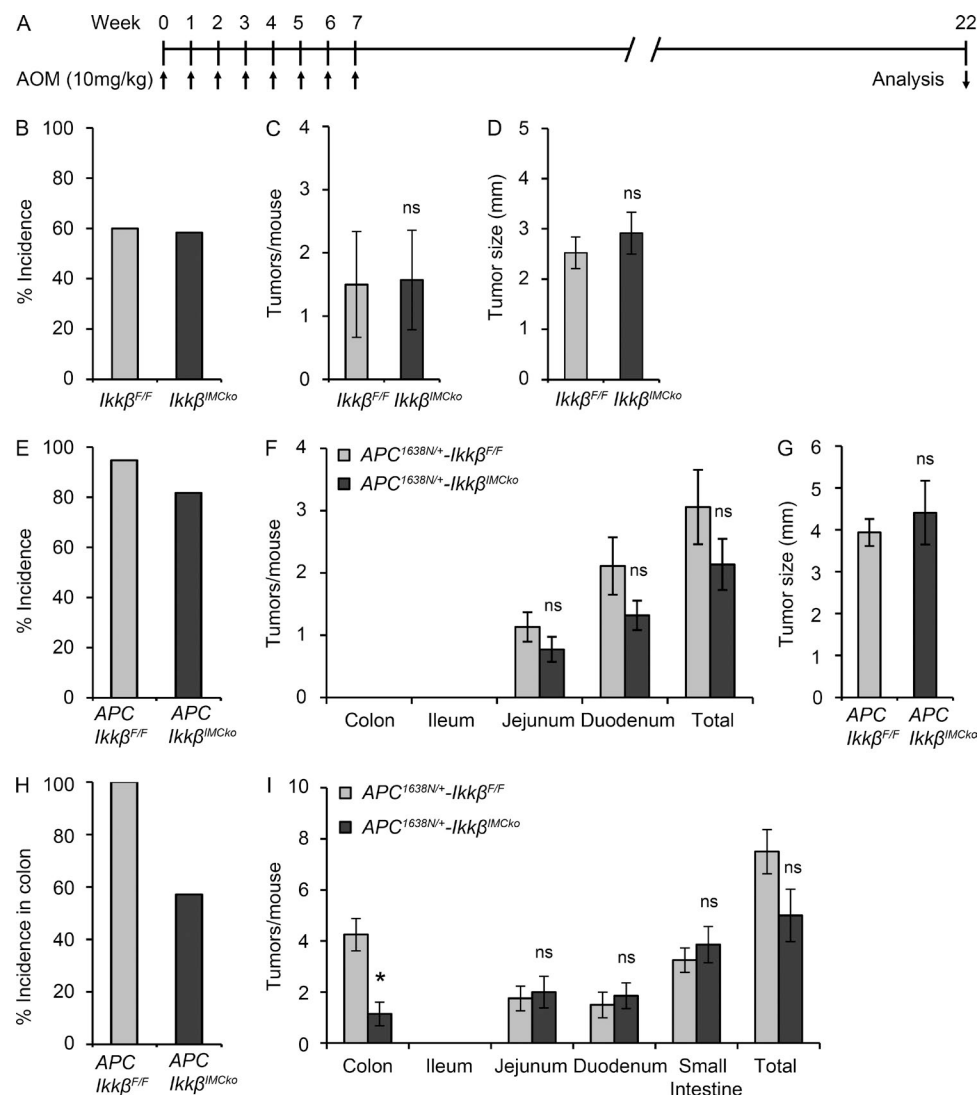
Figure 2. **Genetic deletion of IKKβ in IMCs inhibits colitis–associated tumorigenesis.** (A) Representative immunoblot analysis of IKKβ protein expression in thioglycolate-elicited peritoneal macrophages (TEPMs), colonic IMCs and IECs, from $Ikk\beta^{F/F}$ (F/F) and $Ikk\beta^{IMCko}$ (IMCko) mice. E-cadherin, α-SMA and F4/80 were used as cell-specific markers. β-Actin was used as loading control. (B) Quantification of IKKβ expression in three independently established colonic IMC cultures after normalization with β-actin (**, P < 0.01, using Student's t test). (C) Representative quantification by FACS analysis of mTomato+ and GFP+ cells in mesenchymal cell cultures from the colon (n = 4 individual cultures). (D) Representative confocal image of mTomato+ and GFP+ cells in mesenchymal cell cultures from the colon (n = 4 individual cultures). Bar, 50 μm. (E) Schematic diagram of the AOM/DSS model of CAC. A single AOM injection (10 mg/kg) is followed by three cycles of 2% DSS administration in the drinking water. (F) Body weight loss of $Ikk\beta^{F/F}$ and $Ikk\beta^{IMCko}$ treated with AOM/DSS. (G) Macroscopically visible tumors were counted, and then (H) tumor size, (I) colon length, and (J) colitis score were measured in $Ikk\beta^{IMCko}$ and $Ikk\beta^{F/F}$ littermate controls at day 60 of the CAC model. (K) Representative images of H&E sections from $Ikk\beta^{F/F}$ and $Ikk\beta^{IMCko}$ mice on day 60. Bar, 200 μm. All data are presented as mean ± SE from one of three individual experiments performed (n ≥ 6 mice per group; *, P < 0.05; **, P < 0.01; ns, nonsignificant, using Student's t test).

Tumors in $Ikk\beta^{IMCko}$ mice had also statistically significant reduced size (Fig. 2 H). Colon length and colitis score did not show any difference at this time point (Fig. 2, I–K). Collectively, these data suggest an important pro-tumorigenic role for IKKβ in IMCs during inflammation-induced colorectal carcinogenesis that affects both multiplicity and size of tumors.

IKKβ deletion in IMCs plays a protumorigenic role only in inflammation–associated intestinal carcinogenesis

To investigate whether IMC-specific deletion of IKKβ had the same effect in tumor development in the absence of tissue damage/inflammation, we performed repeated injections with AOM in the absence of DSS. Mice received eight weekly injections with AOM and were sacrificed 22 wk after the first

Figure 3. **Genetic deletion of IKKβ in IMC inhibits intestinal tumorigenesis only in the presence of tissue damage/inflammation.** (A) Schematic diagram of the repeated AOM injections protocol of intestinal carcinogenesis. Tumor incidence (B), tumor number (C), and size (D) in the colon were measured 22 wk after the first AOM injection. Data are presented as mean ± SE from one of two experiments performed ($n \geq 10$ mice per group; ns, nonsignificant; Student's *t* test). Tumor incidence was monitored (E), macroscopically visible tumors were counted (F), and tumor size was measured (G) in 6-mo-old $Apc^{1638N/+}$-$Ikk\beta^{F/F}$ and $Apc^{1638N/+}$-$Ikk\beta^{IMCko}$ ($n \geq 18$ per genotype; ns, nonsignificant; Student's *t* test). Tumor incidence in the colon (H) and number of tumors (I) throughout the intestine were measured in 6-mo-old $Apc^{1638N/+}$-$Ikk\beta^{F/F}$ and $Apc^{1638N/+}$-$Ikk\beta^{IMCko}$ treated at 3 mo of age with 2% DSS for a week. Data are presented as mean ± SE from one of two experiments performed ($n \geq 5$ mice per group; *, P < 0.05; ns, nonsignificant, Student's *t* test).

injection (Fig. 3 A). There was no difference in tumor incidence, number, and size in the colon (Fig. 3, B–D). Similar results were obtained when $Ikk\beta^{IMCko}$ mice were crossed with $Apc^{1638N/+}$ mice. $Apc^{1638N/+}$ mice carry a targeted mutant allele at the endogenous adenomatous polyposis coli (Apc) gene and represent an in vivo model of intestinal tumorigenesis, reminiscent of familial adenomatous polyposis (FAP; Fodde et al., 1994). 6-mo-old $Apc^{1638N/+}$-$Ikk\beta^{IMCko}$ mice showed no difference in tumor incidence, number, or size in comparison to their littermate $Apc^{1638N/+}$-$Ikk\beta^{F/F}$ mice (Fig. 3, E–G). In this model, tumors appear mainly in the upper small intestine.

We then treated $Apc^{1638N/+}$-$Ikk\beta^{IMCko}$ mice with DSS for 7 d when they were 3-mo-old and analyzed tumor development at 6 mo of age. DSS administration in this model accelerates tumor development in the colon (Cooper et al., 2001). We show that only 57% of the $Apc^{1638N/+}$-$Ikk\beta^{IMCko}$ had tumors in contrast to 100% penetrance in control $Apc^{1638N/+}$-$Ikk\beta^{F/F}$ mice (Fig. 3 H). Moreover, the number of tumors in the colon of $Apc^{1638N/+}$-$Ikk\beta^{IMCko}$ mice was significantly lower (Fig. 3 I). These results suggest that tissue damage and/or inflammation are required for IMC-specific IKKβ to act in a protumorigenic manner.

Deletion of IMC–specific IKKβ reduces colitis during the initiation stage of CAC

Because IKKβ acts in a protumorigenic manner only in the presence of colitis, we next hypothesized that IKKβ could influence colitis development early during CAC. We analyzed phenotypic characteristics at early time points during the AOM/DSS treatment, on days 10, 13, and 15 after AOM injection (Fig. 2 E). Day 10 is at the end of the first DSS cycle, and marks the initiation of inflammation and tissue damage. Day 13 corresponds to the time point of maximal weight loss and higher colitis score after the first DSS cycle and is reminiscent of acute DSS colitis. On day 15, weight is usually restored, and thus this day represents an initial restoration phase after the first DSS cycle and an initiation step for tumor development. Histological examination at day 10 showed low colitis score in both $Ikk\beta^{IMCko}$ and $Ikk\beta^{F/F}$ mice (Fig. 4, A and C) On days 13 and 15, the colon of $Ikk\beta^{IMCko}$ mice exhibited significantly less colitis (Fig. 4, A and C), as well as less dysplasia on day 15 (Fig. 4, A and D). These findings correlate well with the increased colon length of $Ikk\beta^{IMCko}$ mice at both the later time points (Fig. 4 B). These data demonstrate that IKKβ in IMCs affects the early stages of CAC, as its deletion leads to reduced colitis and concomitant dysplasia development.

Deletion of IMC–specific IKKβ leads to amelioration of DSS colitis

The results from the early time point experiments suggest that IKKβ in IMCs has also a role in acute DSS colitis. To address this, we performed acute DSS colitis experiments. We found that $Ikk\beta^{IMCko}$ mice lost less weight during the experimental protocol (Fig. 4 E) and had increased colon length at the end (Fig. 4 F). Histologically, $Ikk\beta^{IMCko}$ mice displayed lower colitis score (Fig. 4, G and H). These data are in agreement with the results from $Ikk\beta^{IMCko}$ mice during the first cycle of the AOM/DSS regimen and further reinforce the hypothesis that deletion of IKKβ in IMCs plays a protective role during the first colitis-dependent stage of tumor development in the AOM/DSS model of CAC.

IKKβ in IMCs affects proliferation and apoptosis in the intestine upon damage

To further understand the mechanisms involved in the ameliorated early colitis and subsequent reduced carcinogenesis in the $Ikk\beta^{IMCko}$ mice, we analyzed mechanisms involved in basic cellular functions in the intestine, such as apoptosis and epithelial cell proliferation. To study apoptosis, we performed TUNEL assay in colon tissue and found that cell death was significantly less in $Ikk\beta^{IMCko}$ mice on days 13 and 15 after AOM administration (Fig. 5, A and B). IEC proliferation, measured by BrdU staining was also reduced on both days 13 and 15 (Fig. 5, A and C). Neither apoptosis nor proliferation was different between $Ikk\beta^{F/F}$ and $Ikk\beta^{IMCko}$ mice before induction of the experimental protocol (unpublished data). These results correlate with the histological findings, as decreased cell death reflects the reduced tissue damage we

observe upon DSS administration, which in turn indicates a lower need for compensatory proliferation. The lack of uncontrolled proliferation is associated with reduced dysplasia during the restoration phase of the first DSS cycle and affects later tumor development.

IKKβ in IMCs regulates inflammatory cell infiltration and cytokine production in the intestine
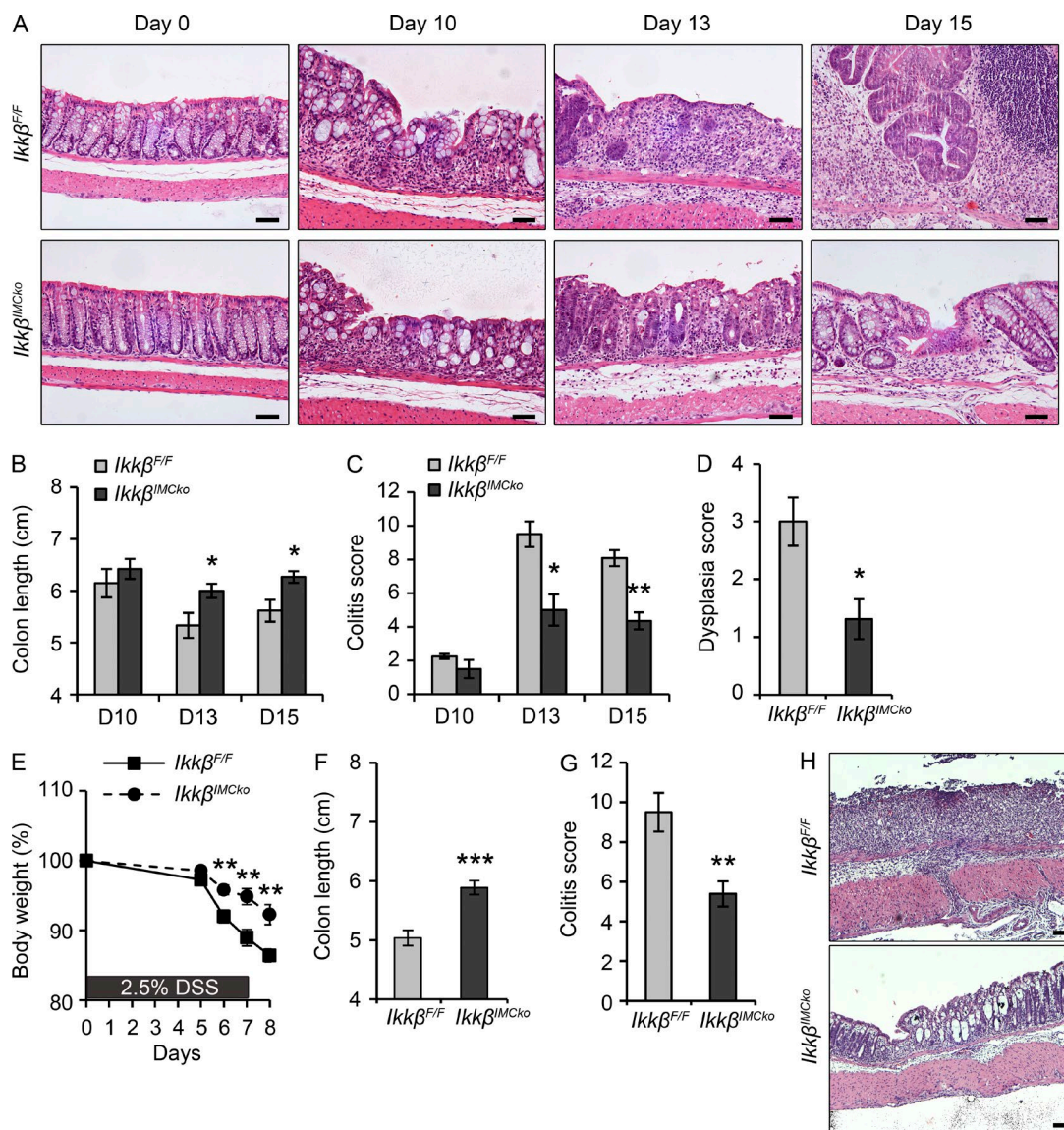
In addition to the histological analysis, we examined in detail the differences in the infiltration of specific inflammatory cell populations during the course of CAC. We performed immunohistochemical staining of colon tissue and found that infiltration of F4/80$^+$ macrophages, Gr1$^+$ neutrophils, B220$^+$ B cells, and CD3$^+$ lymphocytes was significantly reduced in $Ikk\beta^{IMCko}$ mice on days 13 and 15, whereas on day 60 only F4/80$^+$ cells were fewer in $Ikk\beta^{IMCko}$ mice in comparison to their littermate controls (Fig. 6, A and B).

We also found decreased expression of several proinflammatory mediators in colons from $Ikk\beta^{IMCko}$ mouse during the initiation of CAC. We found decreased secretion of the chemokine MIP2 and the cytokines IL-6 and TNF in whole-colon culture supernatants on days 13 and 15 of CAC, decreased production of cyclooxygenase 2 (COX2) in whole-colon extracts and reduced matrix metalloproteinase-9 (MMP9) secretion in organ culture supernatants at the same time points (Fig. 6, C–E). These data indicate that IKKβ in IMCs regulates immune cell infiltration in the intestine upon damage. Moreover, they suggest that altered inflammatory cell infiltration due to ablation of IKKβ in IMCs plays an important role during the initiation stage of the disease rather than the already established tumors, implying a role for naive IMCs rather than CAFs in the regulation of inflammation during CAC in the intestine.

Defective innate immune signaling in IKKβ–deficient IMCs

To investigate whether the differences we observed in $Ikk\beta^{IMCko}$ mice during the initiation of CAC were a result of the presence of a lower number of IMCs—caused either by an intrinsic inability to differentiate and expand or by increased cell death—we performed immunohistochemical staining for α-SMA and Vimentin and Masson's trichrome staining. α-SMA is a marker of activated myofibroblasts and CAFs, vimentin of both fibroblasts and myofibroblasts, whereas Masson's trichrome stains collagen fibers (Fig. 7, A and B). We could not detect any differences between $Ikk\beta^{IMCko}$ mice and their littermate controls either at homeostasis or late in the experimental protocol inside tumors (Fig. 7, A and B), which leads to the conclusion that IKKβ knockout in IMCs does not affect their survival and differentiation during CAC.

We next hypothesized that IKKβ–deficient IMCs could differentially respond to exogenous stimuli caused by defective NF-κB signaling, thus regulating the secretion of mediators that act in a paracrine manner to control inflammation and epithelial transformation. To evaluate this hypothesis, we isolated IMCs from $Ikk\beta^{F/F}$ and $Ikk\beta^{IMCko}$ mice and treated

2240

IKKβ in intestinal mesenchymal cells promotes CAC | Koliaraki et al.

Figure 4. **IMC–specific IKKβ deletion reduces colitis during the early stages of the AOM/DSS and the acute DSS protocol.** (A) Representative images of H&E-stained sections from *Ikkβ^F/F* and *Ikkβ^IMCko* mice on days 0, 10, 13 and 15 after AOM administration. Bars, 50 µm. (B) Colon length was measured on days 10, 13, and 15 after AOM administration. Histopathology scores evaluating (C) colitis and (D) dysplasia in *Ikkβ^F/F* and *Ikkβ^IMCko* mice on days 10, 13, and 15 after AOM administration. (E) Body weight loss of *Ikkβ^F/F* and *Ikkβ^IMCko* during acute DSS colitis. (F) Colon length and (G) colitis score were measured at day 8 after DSS administration. (H) Representative images of H&E-stained sections from *Ikkβ^F/F* and *Ikkβ^IMCko* mice at day 8 after DSS administration. Bars, 100 µm. Data represent mean ± SE from one of three experiments performed ($n \geq 5$ mice per group; *, $P < 0.05$; **, $P < 0.01$; ***, $P < 0.001$, Student's *t* test).

them with common NF-κB inducers, such as LPS, IL-1β, and TNF. We found that IKKβ-deficient IMCs produced less MIP2, TNF, and IL-6 after LPS stimulation (Fig. 7 C). TNF induced MIP2 and IL-6 to a lower extent and showed a decrease in IL-6 production after 24 h. No difference could be seen after IL-1β stimulation, which induced only IL-6—from the tested cytokines—in IMCs (Fig. 7 C). IKKβ-deficient IMCs also produced less COX2 and secreted less MMP9 (Fig. 7, D and E) after LPS, but not TNF or IL-1β treatment. All the mediators we measured in vitro were also differentially

expressed in vivo during the early stages of CAC. Consistent with these results, we also found that IKKβ-deficient IMCs displayed a significant defect in NF-κB activation in response to LPS, as assessed by decreased cytoplasmic IκBα degradation (Fig. 8, A and B), p65 translocation to the nucleus (Fig. 8, A and C), and NF-κB–binding activity (Fig. 8 D). We also observed a similar, though less pronounced defect after stimulation with TNF, whereas no difference could be seen during treatment with IL-1β, consistent to what has been previously published (Fig. 8, A–D; Li et al., 1999; Schmidt-Supprian et
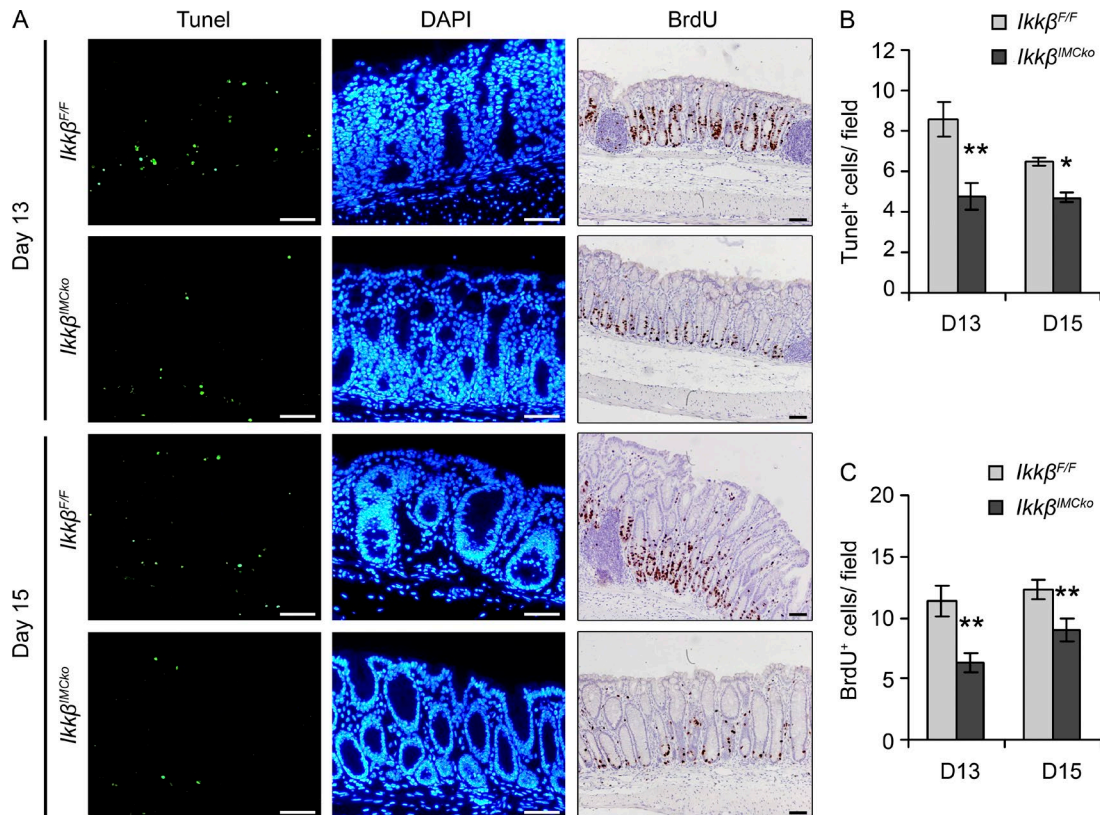
Figure 5. **IMC–specific IKKβ deletion reduces epithelial cell proliferation and apoptosis at the early stages of CAC.** (A) Representative images of TUNEL and BrdU staining of colon sections from *Ikkβ^{F/F}* and *Ikkβ^{IMCko}* mice on days 13 and 15 after AOM administration. DAPI was used to stain nuclei in the TUNEL assay. Quantification of (B) TUNEL⁺ cells per field and (C) BrdU⁺ cells per crypt using at least 10 random fields and 20 random crypts, respectively. Data are presented as mean ± SE (n ≥ 6 mice per genotype from three individual experiments; *, P < 0.05; **, P < 0.01, using Student's t test). Bars, 50 µm.
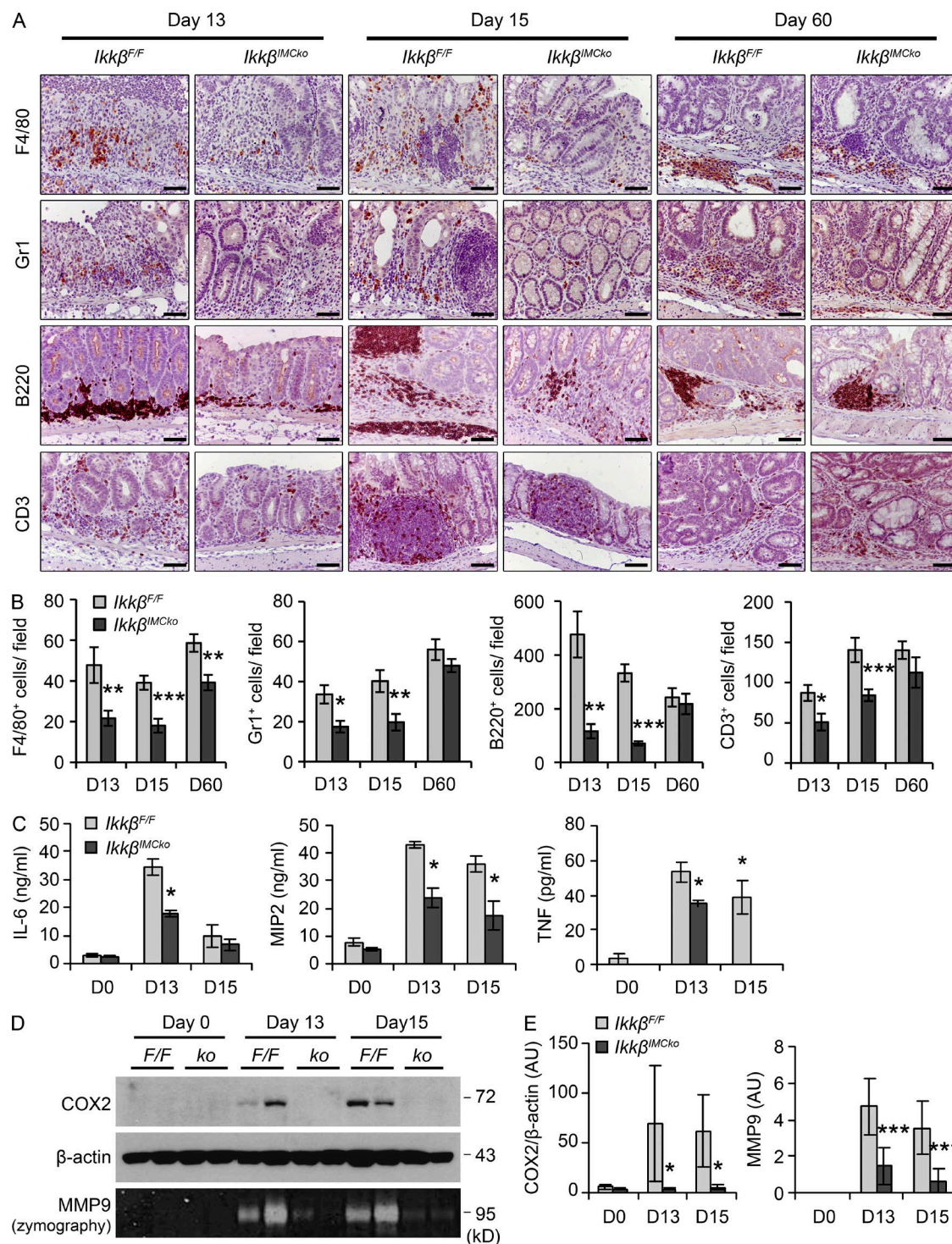
al., 2000). In both LPS and TNF stimulations, differences were more prominent in the translocation of p65 to the nucleus and NF-κB–binding activity, rather than IκBα degradation. We believe that this is a result of the fact that IMC cultures contain ∼50–60% ColVI⁺ cells, leading to 50–60% IKKβ deletion, thus containing a large number of cells that respond normally to these stimulants. In the case of LPS induction, this is further amplified by the relatively low IκBα degradation that it is detected in IMCs in comparison to IL–1β and TNF stimulation, although induction of NF-κB target genes is abundant (Fig. 7 C). Our results, therefore, show that IKKβ in IMCs regulates the production of important mediators of both inflammation and neoplastic transformation in response to innate immune signals.

Soluble mediators from IMCs activate signaling pathways in paracrine epithelial cells

From the examined deregulated cytokines, IL-6 has been causally linked to IEC transformation and the development of colorectal cancer and represents a key link between inflammation and tumorigenesis (Terzić et al., 2010). IL-6 binds to its receptor, a dimer of IL-6R and gp130, and induces the phosphorylation and activation of the transcription factor

STAT3. STAT3 is often found activated in human tumors, including colorectal tumors, by signals from the microenviroment, mainly cytokines and growth factors (Yu et al., 2009). Experiments using animal models of CAC have established the role of both IL-6 and STAT3 in this disease setting (Becker et al., 2004; Bollrath et al., 2009; Grivennikov et al., 2009). Consistent with these previously published data and the decreased IL-6 production in *Ikkβ^{IMCko}* mice early during the disease, we also found a significant decrease in STAT3 phosphorylation (Fig. 9, A and B) in whole-colon extracts from *Ikkβ^{IMCko}* mice on days 13 and 15 after AOM administration. We performed immunohistochemical staining for p-STAT3 in colon tissue and found that this reduction could be seen both in neoplastic cells and cells in the lamina propria both at early and late stages of the disease (Fig. 9 C). In early stages of disease progression, this reduced STAT3 phosphorylation could reflect the reduced inflammation and tissue damage of *Ikkβ^{IMCko}* mice, and therefore the reduced need for regeneration of the epithelium. Interestingly, in tumors from *Apc^{1638N/+}-Ikkβ^{IMCko}* mice, we could not detect any differences in the activation of STAT3 in comparison to their littermate controls (Fig. 9 C). Also, in homeostatic conditions, phosphorylation of STAT3 in the epithelium was limited,

Figure 6. **Reduced inflammatory cell infiltration and expression of proinflammatory mediators in *Ikkβ*[IMCko] mice.** (A) Representative immunohisto-chemical staining for the macrophage marker F4/80, the neutrophil marker Gr1, the B cell marker B220, and the T cell marker CD3 of colons from *Ikkβ*[F/F] and *Ikkβ*[IMCko] mice (*n* = 6–9 mice per genotype from three individual experiments) at the indicated time points. Bars, 50 µm. (B) Quantification of the number of F4/80, Gr1, B220, and CD3+ cells for each genotype at the indicated time points. Data are presented as mean ± SE of at least 20 fields (*n* = 6–9 mice per genotype from three individual experiments; *, P < 0.05; **, P < 0.01; ***, P < 0.001, using Student's *t* test). (C) MIP2, TNF, and IL-6 production, quantified by ELISA in supernatants from whole-colon cultures from *Ikkβ*[F/F] and *Ikkβ*[IMCko] mice on days 0, 13, and 15 after AOM administration. Data represent mean ± SE from one of three individual experiments performed (*n* = 3; *, P < 0.05, using Student's *t* test). (D) Representative COX2 immunoblot analysis of whole-colon

which could explain the lack of a spontaneous intestinal phenotype in the *Ikkβ*^*IMCko*^ mice, as it seems that a trigger is necessary to activate the pathway (Fig. 9, A–C). To verify STAT3 activation specifically in epithelial cells, we also isolated IECs at day 15 of the experimental protocol and measured STAT3 phosphorylation by Western blot analysis. This experiment further verified the reduced STAT3 activation in IECs from *Ikkβ*^*IMCko*^ mice in comparison to their littermate controls under these experimental settings (Fig. 9, D and E).

We also used conditioned medium from IKKβ-deficient IMCs that were incubated with LPS and treated the epithelial cell line HT-29. We found that LPS stimulation of IMCs increased the activation of the STAT3 signaling pathway in epithelial cells, but this effect was much reduced in IKKβ knockout IMCs (Fig. 9 F). These results suggest that IKKβ in IMCs regulates the expression of important proinflammatory mediators, including IL-6, in the colon, influencing the recruitment of immune cells and the proliferation and neoplastic transformation of epithelial cells through the activation of the transcription factor STAT3. This only happens in the presence of tissue damage and concomitant inflammation, implying that the signals that IMCs respond to come from the damaged and inflamed mucosa, rather than the transforming epithelial cells, at least in the case of colorectal cancer (Fig. 9 G).
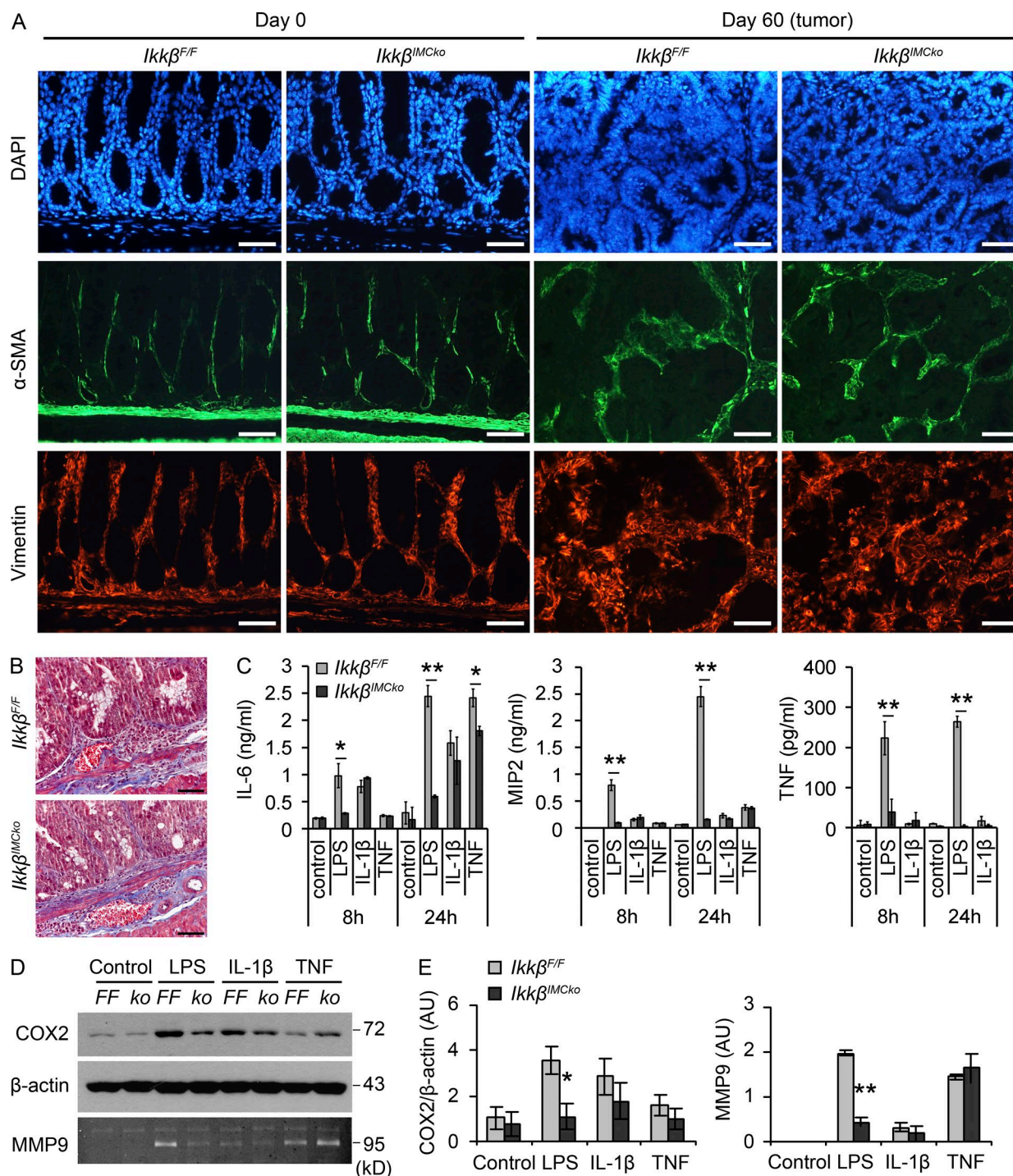
DISCUSSION

Pharmacological inhibition of IKKβ has been shown to confer protection against the AOM/DSS mouse model of inflammation-driven intestinal tumorigenesis (Hayakawa et al., 2009). Cell-specific ablation of IKKβ in either epithelial or myeloid cells is also known to have a protective role in the same model, although through distinct mechanisms of action. On the one hand, deletion of IKKβ in IECs exacerbates DSS colitis through decreased NF-κB–mediated protection against epithelial cell apoptosis and delayed mucosal regeneration, thereby reducing colitis-associated tumorigenesis (Greten et al., 2004; Eckmann et al., 2008). On the other hand, IKKβ in myeloid cells affects tumor multiplicity and size mainly through the regulation of proinflammatory mediator and growth factor production (Greten et al., 2004). In this study, we show that IMC-specific deletion of IKKβ also confers protection in the AOM/DSS mouse model, contributing to the overall antitumorigenic effect that IKKβ inhibition exerts in this model. Mesenchymal IKKβ acts through the regulation of proinflammatory and protumorigenic mediator production, which affects the recruitment of immune cells and the proliferation and neoplastic transformation of epithelial cells early during the tumorigenic process, in a manner surprisingly similar to that of myeloid-specific IKKβ.

An important mechanism of the protumorigenic function of IKKβ in IMCs appears to be through the regulation of inflammation and, specifically, the production of proinflammatory cytokines and chemokines, including IL-6. It was recently shown that CAFs from skin, mammary, and pancreatic tumors play a role in tumorigenesis through an IKKβ-dependent proinflammatory gene signature, including IL-6, which affects the recruitment, activation, and function of inflammatory cells (Erez et al., 2010; Servais and Erez, 2013). Our study shows, using in vivo genetic approaches and disease models that a similar mechanism functions in CAC, but acts predominantly in stroma fibroblasts associated with early preCAF stages of tumor development. Indeed, mesenchymal IKKβ deletion is also sufficient to ameliorate tissue damage and inflammation in the DSS model of colitis. Interestingly, a recent study has shown that IL-6 is strongly expressed in intestinal myofibroblasts in both untreated and DSS-treated mice and contributes to disease progression (Shaker et al., 2014). IL-6 is especially important, as it triggers STAT3 phosphorylation and activation in epithelial cells, a crucial protumorigenic molecular pathway in the intestine (Becker et al., 2004; Bollrath et al., 2009; Grivennikov et al., 2009). Besides IL-6, other proinflammatory molecules are also decreased, reducing immune cell infiltration, which in turn can reduce total cytokine/chemokine levels in the tissue, creating a feedback loop.

Interestingly, IKKβ deletion in IMCs has no effect on tumor development in the APC model of spontaneous intestinal tumorigenesis, implying that this pathway in the intestine functions in the early activated fibroblasts rather than the CAFs. It also suggests that the early damaged and inflamed mucosa microenvironment rather than the tumor mass instructs fibroblasts to act in a protumorigenic fashion. Moreover, mice that lack IKKβ in IMCs do not exhibit any spontaneous intestinal phenotype. In fact, during homeostasis, intestinal inflammatory mediator expression, inflammatory cell infiltration, and STAT3 activation are very low and comparable to that of littermate controls, providing further evidence for the need of a stimulus that triggers the proinflammatory/protumorigenic role of IKKβ in IMCs. Thus, these findings prompt another important question: what is the source of the signals that make IMC-specific IKKβ protumorigenic under these conditions? IKKβ lies downstream of major proinflammatory pathways, including TLRs, TNFR, and IL-1R family. So far, molecules from nearby immune and cancer cells, like IL-1β, have been implicated in this "reprogramming" of normal fibroblasts (Erez et al., 2010). Our ex vivo data support the idea that IKKβ in IMCs regulates the production of important mediators of both inflammation and neoplastic transformation in response to innate immune signals, as IKKβ-deficient primary cells show defective NF-κB activation

---

lysates and MMP9 zymography detection in supernatants from whole-colon cultures from *Ikkβ*^*F/F*^ (*F/F*) and *Ikkβ*^*IMCko*^ (*ko*) mice at the same time points. β-Actin was used as loading control. Data represent one of three experiments performed. (E) Quantification of COX2 and MMP9 band intensity. COX2 is expressed relative to β-actin. Data represent mean ± SE (n = 5–8 mice per group from three independent experiments; *, P ≤ 0.05; ***, P ≤ 0.001, Student's t test).

Figure 7. **IKKβ–deficient mesenchymal cells display a defective response to innate immune signals.** (A) Representative immunohistochemical staining for α-SMA and vimentin on colon sections from $Ikkβ^{F/F}$ and $Ikkβ^{IMCko}$ mice at the indicated time points ($n = 6$ per genotype from two individual experiments). DAPI was used to stain nuclei. Bars, 50 µm. (B) Representative Masson's trichrome staining of colon sections from $Ikkβ^{F/F}$ and $Ikkβ^{IMCko}$ mice at day 60 of the AOM/DSS protocol ($n = 6$ per genotype from two individual experiments). Bars, 50 µm. (C) IL-6, MIP2, and TNF were measured by ELISA in supernatants from $Ikkβ^{F/F}$ and $Ikkβ^{IMCko}$ primary IMC cultures before and after induction with LPS (1 µg/ml), IL-1β (10 ng/ml), and TNF (10 ng/ml) for 8 and 24 h. Data represent mean ± SE of one from three experiments performed in triplicates. (*, $P ≤ 0.05$; **, $P < 0.01$, using Student's t test). (D) COX2 was detected in protein lysates from $Ikkβ^{F/F}$ (FF) and $Ikkβ^{IMCko}$ (ko) primary IMC cultures before and after induction with LPS, IL-1β, and TNF for 24 h. MMP9 activity was detected in culture supernatants by zymography. Data represent one of three experiments performed. (E) Quantification of COX2 and MMP9 band intensity. COX2 is expressed relative to β-actin. Data represent mean ± SE ($n = 3$ independent experiments; *, $P ≤ 0.05$; **, $P ≤ 0.01$, Student's t test).
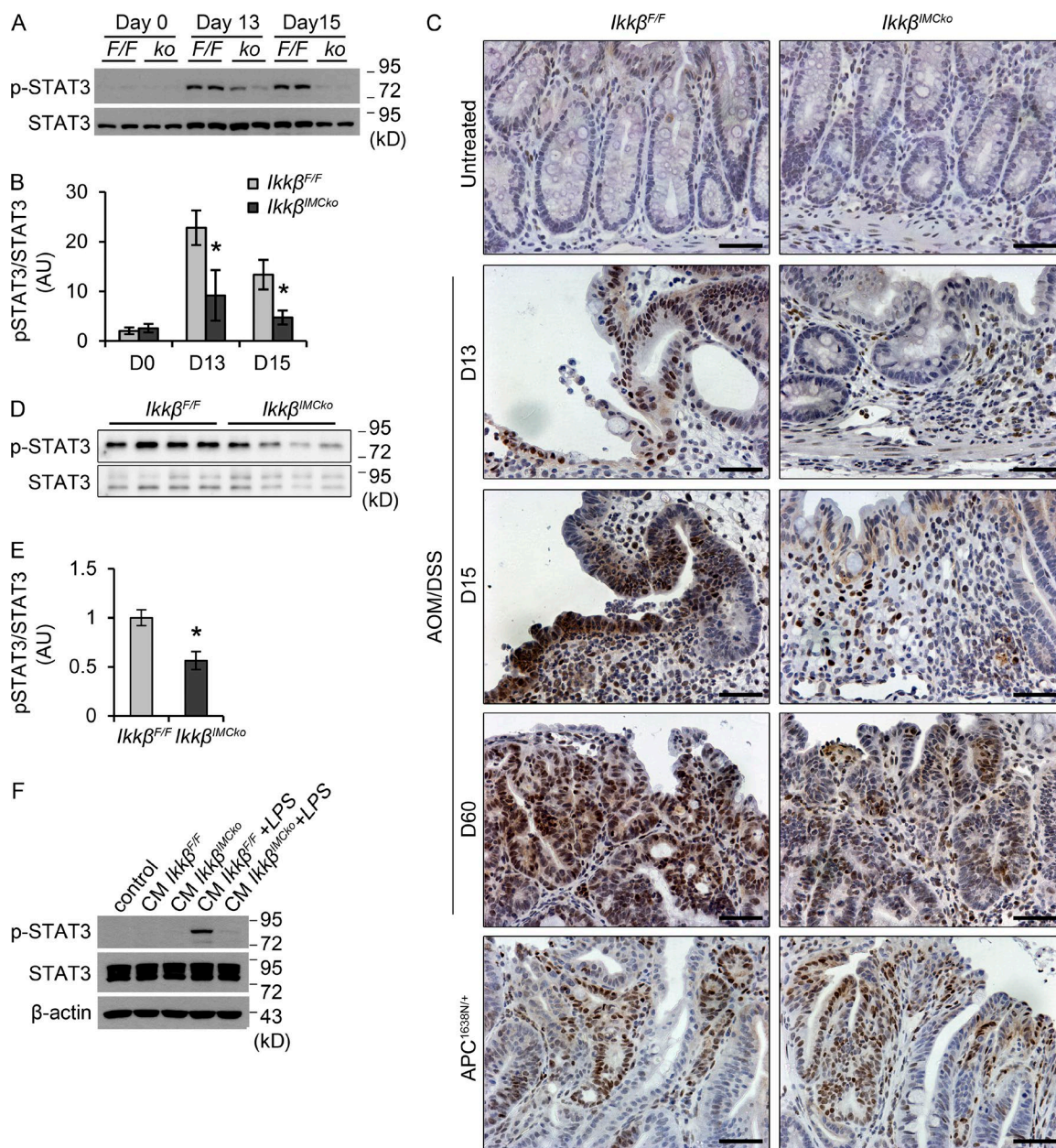
Figure 8.   IKKβ–deficient mesenchymal cells display defective NF-κB activation in response to innate immune signals. (A) Representative immunoblot detection of IκBα in cytoplasmic extracts and p65 in nuclear extracts from *Ikkβ^F/F* and *Ikkβ^IMCko* primary IMC cultures before and after induction with LPS, IL-1β, and TNF at the indicated time points. β-Actin and lamin A/C were used as loading controls, respectively. (B) Quantification of IκBα band intensity. IκBα is expressed relative to β-actin. (C) Quantification of p65 band intensity. p65 is expressed relative to lamin A/C. (D) Detection of NF-κB binding activity in nuclear extracts from *Ikkβ^F/F* and *Ikkβ^IMCko* primary IMC cultures before and after induction with LPS, IL-1β, and TNF at the indicated time points. Data represent mean ± SE (n = 3 independent experiments; *, P ≤ 0.05; **, P ≤ 0.01, ns = nonsignificant, using Student's t test).

and concomitant chemokine/cytokine production in response to TNF and LPS, but not IL-1β. This is further supported by the fact that complete TLR4 knockout mice are also protected from AOM/DSS–induced tumorigenesis (Fukata et al., 2007) and experiments using bone marrow transfers have shown that TLR4 in the stromal compartment is necessary for the development of tumors, although the contribution of mesenchymal cells has not been addressed (Fukata et al., 2009, 2011). TNF is another possible candidate for NF-κB activation in IMCs and previous work from our laboratory has shown that IMCs are primary targets for pathogenic TNF and

sufficient for the development of TNF-dependent Crohn's-like ileitis (Armaka et al., 2008). However, experiments of bone marrow chimeras using the AOM/DSS model of CAC have shown that TNFR1 deletion leads to amelioration of the CAC phenotype predominantly through its function on hematopoietic cells (Popivanova et al., 2008).

Mesenchymal cells in the intestine are a diverse set of cell types that are not yet well characterized (Mifflin et al., 2011). Mesenchymal cells in the tumors, namely CAFs, usually originate from multiple sources, including the resident mesenchymal pool (Kalluri and Zeisberg, 2006). In our

Figure 9. **Reduced STAT3 phosphorylation in *Ikkβ^IMCko^* mice during CAC.** (A) Representative p-STAT3 immunoblot analysis of whole-colon lysates from *Ikkβ^F/F^* (*F/F*) and *Ikkβ^IMCko^* (*ko*) mice at the indicated time points. Total STAT3 was used as loading control. Data represent one of three experiments performed. (B) Quantification of p-STAT3 immunoblot band intensity. p-STAT3 is expressed relative to total STAT3. Data represent mean ± SE (*n* = 3 mice per group from 3 independent experiments; *P ≤ 0.05, using Student's *t* test). (C) Representative immunohistochemical staining for p-STAT3 on colon sections from *Ikkβ^F/F^* and *Ikkβ^IMCko^* mice (*n* = 6–9 per genotype from 3 individual experiments) at the indicated time points. Bars, 50 μm. (D) Representative p-STAT3 immunoblot analysis of IECs isolated from *Ikkβ^F/F^* and *Ikkβ^IMCko^* mice at day 15 of the AOM/DSS experimental protocol. Total STAT3 was used as loading control. Data represent one of two experiments performed. (E) Quantification of p-STAT3 immunoblot band intensity. p-STAT3 is expressed relative to total STAT3. Data represent mean ± SE (*n* = 4–5 mice per group from two independent experiments; *, P ≤ 0.05, using Student's *t* test). (F) Immunoblot analysis of p-STAT3 in HT-29 epithelial cell line after incubation with conditioned medium (CM) from *Ikkβ^F/F^* and *Ikkβ^IMCko^* IMCs treated with LPS (1 μg/ml) for 8 h. Data are representative of one from three experiments performed.

study, we show that the mesenchymal cells that are targeted by the ColVI-cre mouse and display defective immune activation in the absence of IKKβ, refer to a subpopulation of vimentin⁺ColV⁺ fibroblasts and myofibroblasts/pericytes that give rise to a small fraction of activated CAFs during carcinogenesis. Although the fact that the ColVI-cre mouse does

not target all fibroblasts could be explained by nonefficient recombination, we believe that the uniform network-like distribution of ColVI-GFP^{+} cells and the presence of a robust and significant phenotype in colitis and CAC in our study point to the specificity of our Cre system for a subpopulation of fibroblasts in the intestine, which awaits more detailed characterization.

Interestingly, a study by Pallangyo et al. (in this issue) shows that deletion of IKKβ in mesenchymal cells driven by the Col1a2CreER mouse in the intestine upon tamoxifen administration leads to increased tumor size in the AOM/DSS model of colitis-induced tumorigenesis. Although this may seem contradictory at first, we believe that differences in the mesenchymal subpopulations targeted in each case are the reason for the different phenotypes observed and the different underlying mechanisms proposed. An initial analysis of the specificity of each Cre-line shows that the Col1a2creER targets a much larger mesenchymal cell population than the ColVIcre mouse, both in homeostasis and in tumors. Moreover, deletion of IKKβ with ColVIcre affects mainly the early stages of colitis-induced tumorigenesis, whereas with Col1a2creER, no difference can be seen in weight loss and histological score at these time points. Interestingly, cytokine (IL-6) and chemokine expression (Cxcl1, Cxcl12) is decreased in fibroblasts with a Col1a2cre-mediated deletion of IKKβ, implying an effect of mesenchymal NF-κB in inflammatory gene signatures, which is not reflected in the phenotype. These two studies further demonstrate the need for a better characterization of the identities and different functions of mesenchymal cells in the intestine and their relative contribution to carcinogenesis. It also becomes evident that a thorough understanding of the different subpopulations of mesenchymal cells in the intestine is crucial in understanding their function and devising ways to target them therapeutically.

Collectively, our data show that IKKβ in IMCs has a tumor-promoting role in the AOM/DSS model of CAC. IMCs or, more accurately, a subpopulation of these cells sense tissue damage and respond to produce proinflammatory and tissue-remodeling molecules. These secondary signals attract and activate inflammatory cells establishing a proinflammatory milieu in the microenviroment and further support neoplastic cell proliferation through downstream activation of the STAT3 signaling pathway, thus promoting tumor development.

MATERIALS AND METHODS

Mice. *Ikkβ^{F/F}* mice and Tg(CollagenVI-Cre) mice were previously described (Pasparakis et al., 2002; Armaka et al., 2008). ROSA^{mTmG} mice were purchased from The Jackson Laboratory (Muzumdar et al., 2007). Mice were maintained on a C57BL/6J genetic background, and experimental groups contained littermates that were caged together according to gender. Experiments were performed in the conventional unit of the animal facilities in Biomedical Sciences Research Center (BSRC) "Alexander Fleming" under specific pathogen–free conditions, in accordance with the guidance of the Institutional Animal Care and Use Committee of BSRC "Alexander Fleming."

Induction of colitis and CAC. Induction of DSS colitis and CAC was performed as previously described (Neufert et al., 2007; Wirtz et al., 2007). In brief, DSS colitis was induced in 6–8-wk-old mice with 2.5% DSS (MW: 36,000–50,000 D; MP Biomedicals) added in the drinking water for 7 d, followed by 1 d of normal water. For CAC, mice were injected i.p. with 10 mg/kg AOM (Sigma-Aldrich). 5 d later, 2% DSS was added in the drinking water for 5 d, and this was repeated for two additional cycles with an interval of 16 d between each cycle. At day 60, colon was removed and macroscopically visible tumors were counted. Assessment of histopathological scores was performed on formalin-fixed, paraffin-embedded (FFPE) colon sections after staining with hematoxylin (Sigma-Aldrich) and eosin (Sigma-Aldrich), as previously described (Koliaraki et al., 2012). Staining with Masson's trichrome was performed according to manufacturer's instructions (Sigma-Aldrich).

FACS analysis for the characterization of ColVIcre–mT/mG mice. Colon and/or small intestine from ColVIcre-mT/mG mice was removed, cut into 0.5–1 cm pieces, and extensively washed with HBSS (Invitrogen). The tissue was then incubated in HBSS containing 5 mM EDTA and 1 mM dithiothreitol (DTT) for 10 min at 37°C to partly remove epithelial cells. This was followed by incubation with 300 U/ml Collagenase XI (Sigma-Aldrich), 0.1 mg/ml Dispase (Roche), and 50 U/ml DNase (Sigma-Aldrich) in DMEM (Biochrom) for 90 min at 37°C. The resulting cell suspension was stained with antibodies against CD45 (BioLegend), CD31 (BD), Ter-119 (eBioscience), E-Cadherin (BD), CD140α (eBioscience), CD140β (eBioscience), CD44 (eBioscience), and CD29 (eBioscience). For intracellular staining, cells were fixed and permeabilized using the Fixation and Permeabilization Buffer Set (eBioscience) according to manufacturer's instructions. Cells were then stained with primary antibodies against Vimentin (Abcam) and Collagen IV (Abcam), followed by secondary anti–rabbit Alexa Fluor 647–conjugated antibody (Invitrogen) at room temperature. FACS analysis was performed with a FACSCantoII flow cytometer (BD) and FACSDiva (BD) or FlowJo software (FlowJo, LLC).

Immunohistochemistry and immunofluorescence. FFPE colon sections were probed with antibodies against F4/80 (AbD Serotec), Gr-1 (AbD Serotec), CD3 (Abcam), B220 (BD), p-STAT3 (Cell Signaling Technology), Vimentin (Abcam), and α-SMA (FITC-conjugated; Sigma-Aldrich). The anti–rabbit Alexa Fluor 568–conjugated secondary antibody (Invitrogen), biotinylated secondary antibodies (Vector Laboratories), the Vectastain ABC kit (Vector Laboratories), and the Vectastain DAB kit or the Vectastain NovaRED kit (Vector Laboratories), were used for signal amplification and detection. Images were acquired with an Eclipse E800 microscope

(Nikon) equipped with a Dxm1200F camera (Nikon). Cryosections of paraformaldehyde (PFA)-fixed tissue samples or PFA-fixed cells were probed with antibodies against Vimentin (Abcam), α-SMA (Sigma-Aldrich), and Collagen IV (Abcam), followed by secondary antibodies conjugated with Alexa Fluor 647 (Invitrogen). Images were acquired with a TCS SP8X White Light Laser confocal system (Leica).

Assessment of proliferation and apoptosis. To determine proliferation, mice were injected i.p. with 100 mg/kg BrdU (Sigma-Aldrich) 2 h before sacrifice. FFPE tissue sections were stained with the BrdU detection kit (BD). The number of BrdU$^+$ cells was quantified in at least 20 intact, well-orientated crypts per mouse. Apoptosis was evaluated using the DeadEnd Fluorometric Tunel system (Promega) in tissue sections. DAPI (Santa Cruz Biotechnology, Inc.) was used to stain the nuclei. The number of Tunel$^+$ cells was quantified in at least 10 random fields in each slide.

Isolation of IMCs and cell culture. For isolation of IMCs, colons from 5–8-wk-old mice were removed, cut in 0.5–1 mm pieces and washed with HBSS (Invitrogen). Intestinal pieces were then incubated in HBSS containing 5 mM EDTA and 1 mM DTT for 20 min at 37°C to remove the epithelial layer. This was followed by incubation with 300 U/ml Collagenase XI (Sigma-Aldrich) and 0.1 mg/ml Dispase (Roche) in DMEM (Biochrom) for 60 min at 37°C. Supernatants were centrifuged and cell pellets were resuspended in DMEM supplemented with 10% FBS (Biochrom), 1% nonessential amino acids (Sigma-Aldrich), 100 U/ml penicillin, 100 µg/ml streptomycin, and 1 µg/ml amphotericin B (Sigma-Aldrich) and plated in cell culture flasks. At passages 3–4, cells were treated with 10 ng/ml IL-1β (PeproTech) or 1 µg/ml LPS (Sigma-Aldrich) or 10 ng/ml TNF (provided by C. Libert, Ghent University, Belgium) for the indicated time points. For experiments with conditioned medium (CM), cells were plated, serum starved, and then induced with LPS (1 µg/ml) for 8 h. Cells were then washed with PBS and serum-free DMEM and fresh DMEM was added for 48 h. The supernatant was then collected, passed through a 0.2-µm pore size filter, and stored at −80°C. The CM was added on HT-29 epithelial cells for 15 min in a ratio of 1:1 with serum-free DMEM.

Isolation of IECs. IEC isolation was performed as previously described (Koliaraki et al., 2012). In brief, colon was extensively washed with HBSS supplemented with 2% FBS and antibiotics, followed by incubation in HBSS/2% FBS, containing 1 mM EDTA and 1 mM DTT at 37°C for 45 min. Cells in the supernatant were layered on a discontinuous 25/40% Percoll gradient (Sigma-Aldrich) and centrifuged at 600 *g* for 10 min, and then IECs were collected from the interphase.

Whole-colon culture and cytokine measurement. Full-thickness organ cultures were performed as previously described (Wirtz et al., 2007). In brief, colon was opened longitudinally

and washed with ice-cold PBS supplemented with 20 µg/ml gentamicin (Sigma-Aldrich). With the use of a punch biopsy instrument, four 4-mm specimens were obtained and placed in 1 ml RPMI-1640 medium (Invitrogen), supplemented with 100 U/ml penicillin, 100 µg/ml streptomycin, and 20 µg/ml gentamicin. Supernatant was collected after 18 h and cytokines were measured using commercially available ELISA kits. ELISAs for MIP2 and IL-6 were purchased from PeproTech and for TNF from eBioscience.

Nuclear extract isolation and NF-κB transcription factor assay. For nuclear extract purification, cells were resuspended in hypotonic solution (10 mM Hepes [pH 7.9], 10 mM KCl, 1.5 mM MgCl$_2$, 0.5 mM DTT, protease inhibitors [Roche], and phosphatase inhibitors [Sigma-Aldrich]), incubated on ice for 15 min and centrifuged at 13,000 rpm for 20 s. The supernatant containing the cytoplasmic fraction was stored and the pellet was resuspended in nuclear extraction buffer containing 20 mM Hepes [pH 7.9], 420 mM NaCl, 1.5 mM MgCl$_2$, 0.2 mM EDTA, 0.5 mM DTT, 25% glycerol, protease inhibitors (Roche), and phosphatase inhibitors (Sigma-Aldrich), incubated for 30 min at 4°C and centrifuged at 13,000 rpm for 5 min. NF-κB–specific transcription factor DNA-binding activity in nuclear extracts was performed using the NF-κB (mouse p65) transcription factor assay kit from Cayman Chemical Co., according to the manufacturer's instructions.

Western blotting and gelatin zymography. Cell or tissue extracts (in RIPA buffer, containing 1% Triton X-100, 1% sodium deoxycholate, 0.1% SDS, 150 mM NaCl, 10 mM Tris HCl, pH 7.4, 1 mM EDTA, protease inhibitors [Roche], and phosphatase inhibitors [Sigma-Aldrich]) were subjected to 10% SDS-PAGE and subsequently transferred to a nitrocellulose membrane (Whatman GmbH). Membranes were probed with antibodies against p-STAT3 (Call Signaling Technology), COX2 (Cayman), STAT3, IκBα, and β-actin (Santa Cruz Biotechnology, Inc.). For detection of MMP9 in cell culture or whole-colon culture supernatants, these were analyzed on 8% SDS-PAGE containing 1 mg/ml gelatin under nonreduced conditions at 4°C. Gels were washed in 2.5% Triton X-100 for 1 h, incubated in MMP activation buffer (50 mM Tris-HCl [pH 7.5], 5 mM CaCl$_2$, 0,02% NaN$_3$, and 1 µM ZnCl$_2$) for 18 h at 37°C and stained with 0.5% Coomassie blue R250. Quantification of bands from Western blot or zymography was performed with ImageJ software (National Institutes of Health).

Statistical analysis. Data are presented as mean ± SE. Student's *t* test was used for evaluation of statistical significance. P-values <0.05 were considered significant.

REFERENCES

Armaka, M., M. Apostolaki, P. Jacques, D.L. Kontoyiannis, D. Elewaut, and G. Kollias. 2008. Mesenchymal cell targeting by TNF as a common pathogenic principle in chronic inflammatory joint and intestinal diseases. *J. Exp. Med.* 205:331–337. http://dx.doi.org/10.1084/jem .20070906

Becker, C., M.C. Fantini, C. Schramm, H.A. Lehr, S. Wirtz, A. Nikolaev, J. Burg, S. Strand, R. Kiesslich, S. Huber, et al. 2004. TGF-beta suppresses tumor progression in colon cancer by inhibition of IL-6 trans-signaling. *Immunity.* 21:491–501. http://dx.doi.org/10.1016/j.immuni.2004.07 .020

Ben-Neriah, Y., and M. Karin. 2011. Inflammation meets cancer, with NF-κB as the matchmaker. *Nat. Immunol.* 12:715–723. http://dx.doi .org/10.1038/ni.2060

Bhowmick, N.A., A. Chytil, D. Plieth, A.E. Gorska, N. Dumont, S. Shappell, M.K. Washington, E.G. Neilson, and H.L. Moses. 2004. TGF-beta signaling in fibroblasts modulates the oncogenic potential of adjacent epithelia. *Science.* 303:848–851. http://dx.doi.org/10.1126/science.1090922

Bollrath, J., T.J. Phesse, V.A. von Burstin, T. Putoczki, M. Bennecke, T. Bateman, T. Nebelsiek, T. Lundgren-May, O. Canli, S. Schwitalla, et al. 2009. gp130-mediated Stat3 activation in enterocytes regulates cell survival and cell-cycle progression during colitis-associated tumorigenesis. *Cancer Cell.* 15:91–102. http://dx.doi.org/10.1016/j.ccr.2009.01.002

Clevers, H. 2004. At the crossroads of inflammation and cancer. *Cell.* 118:671–674. http://dx.doi.org/10.1016/j.cell.2004.09.005

Cooper, H.S., L. Everley, W.C. Chang, G. Pfeiffer, B. Lee, S. Murthy, and M.L. Clapper. 2001. The role of mutant Apc in the development of dysplasia and cancer in the mouse model of dextran sulfate sodium–induced colitis. *Gastroenterology.* 121:1407–1416. http://dx.doi.org/10.1053/gast .2001.29609

DiDonato, J.A., F. Mercurio, and M. Karin. 2012. NF-κB and the link between inflammation and cancer. *Immunol. Rev.* 246:379–400. http:// dx.doi.org/10.1111/j.1600-065X.2012.01099.x

Eckmann, L., T. Nebelsiek, A.A. Fingerle, S.M. Dann, J. Mages, R. Lang, S. Robine, M.F. Kagnoff, R.M. Schmid, M. Karin, et al. 2008. Opposing functions of IKKbeta during acute and chronic intestinal inflammation. *Proc. Natl. Acad. Sci. USA.* 105:15058–15063. http://dx.doi.org/10.1073 /pnas.0808216105

Erez, N., M. Truitt, P. Olson, S.T. Arron, and D. Hanahan. 2010. Cancer-Associated Fibroblasts Are Activated in Incipient Neoplasia to Orchestrate Tumor-Promoting Inflammation in an NF-kappaB–Dependent Manner. *Cancer Cell.* 17:135–147. http://dx.doi.org/10.1016/j.ccr.2009.12.041

Fodde, R., W. Edelmann, K. Yang, C. van Leeuwen, C. Carlson, B. Renault, C. Breukel, E. Alt, M. Lipkin, P.M. Khan, et al. 1994. A targeted chain-termination mutation in the mouse Apc gene results in multiple intestinal tumors. *Proc. Natl. Acad. Sci. USA.* 91:8969–8973. http://dx .doi.org/10.1073/pnas.91.19.8969

Fukata, M., A. Chen, A.S. Vamadevan, J. Cohen, K. Breglio, S. Krishnareddy, D. Hsu, R. Xu, N. Harpaz, A.J. Dannenberg, et al. 2007. Toll-like receptor-4 promotes the development of colitis-associated colorectal tumors. *Gastroenterology.* 133:1869–1881. http://dx.doi.org/10.1053/j.gastro .2007.09.008

Fukata, M., Y. Hernandez, D. Conduah, J. Cohen, A. Chen, K. Breglio, T. Goo, D. Hsu, R. Xu, and M.T. Abreu. 2009. Innate immune signaling by Toll-like receptor-4 (TLR4) shapes the inflammatory microenvironment in colitis-associated tumors. *Inflamm. Bowel Dis.* 15:997–1006. http://dx .doi.org/10.1002/ibd.20880

Fukata, M., L. Shang, R. Santaolalla, J. Sotolongo, C. Pastorini, C. España, R. Ungaro, N. Harpaz, H.S. Cooper, G. Elson, et al. 2011. Constitutive activation of epithelial TLR4 augments inflammatory responses to mucosal injury and drives colitis-associated tumorigenesis. *Inflamm. Bowel Dis.* 17:1464–1473. http://dx.doi.org/10.1002/ibd.21527

Greten, F.R., L. Eckmann, T.F. Greten, J.M. Park, Z.W. Li, L.J. Egan, M.F. Kagnoff, and M. Karin. 2004. IKKbeta links inflammation and tumorigenesis in a mouse model of colitis-associated cancer. *Cell.* 118:285–296. http://dx.doi.org/10.1016/j.cell.2004.07.013

Grivennikov, S., E. Karin, J. Terzic, D. Mucida, G.Y. Yu, S. Vallabhapurapu, J. Scheller, S. Rose-John, H. Cheroutre, L. Eckmann, and M. Karin. 2009. IL-6 and Stat3 are required for survival of intestinal epithelial cells and development of colitis-associated cancer. *Cancer Cell.* 15:103–113. http ://dx.doi.org/10.1016/j.ccr.2009.01.001

Grivennikov, S.I., F.R. Greten, and M. Karin. 2010. Immunity, inflammation, and cancer. *Cell.* 140:883–899. http://dx.doi.org/10.1016/j.cell.2010 .01.025

Hanahan, D., and L.M. Coussens. 2012. Accessories to the crime: functions of cells recruited to the tumor microenvironment. *Cancer Cell.* 21:309–322. http://dx.doi.org/10.1016/j.ccr.2012.02.022

Hanahan, D., and R.A. Weinberg. 2011. Hallmarks of cancer: the next generation. *Cell.* 144:646–674. http://dx.doi.org/10.1016/j.cell.2011 .02.013

Hayakawa, Y., S. Maeda, H. Nakagawa, Y. Hikiba, W. Shibata, K. Sakamoto, A. Yanai, Y. Hirata, K. Ogura, S. Muto, et al. 2009. Effectiveness of IkappaB kinase inhibitors in murine colitis-associated tumorigenesis. *J. Gastroenterol.* 44:935–943. http://dx.doi.org/10.1007/s00535-009 -0098-7

Kalluri, R., and M. Zeisberg. 2006. Fibroblasts in cancer. *Nat. Rev. Cancer.* 6:392–401. http://dx.doi.org/10.1038/nrc1877

Koliaraki, V., M. Roulis, and G. Kollias. 2012. Tpl2 regulates intestinal myofibroblast HGF release to suppress colitis-associated tumorigenesis. *J. Clin. Invest.* 122:4231–4242. http://dx.doi.org/10.1172/JCI63917

Li, Q., D. Van Antwerp, F. Mercurio, K.F. Lee, and I.M. Verma. 1999. Severe liver degeneration in mice lacking the IkappaB kinase 2 gene. *Science.* 284:321–325. http://dx.doi.org/10.1126/science.284.5412.321

Liu, F., Y. Xia, A.S. Parker, and I.M. Verma. 2012. IKK biology. *Immunol. Rev.* 246:239–253. http://dx.doi.org/10.1111/j.1600-065X.2012.01107.x

Mantovani, A., P. Allavena, A. Sica, and F. Balkwill. 2008. Cancer-related inflammation. *Nature.* 454:436–444. http://dx.doi.org/10.1038/ nature07205

Mifflin, R.C., I.V. Pinchuk, J.I. Saada, and D.W. Powell. 2011. Intestinal myofibroblasts: targets for stem cell therapy. *Am. J. Physiol. Gastrointest. Liver Physiol.* 300:G684–G696. http://dx.doi.org/10.1152/ajpgi.00474 .2010

Muzumdar, M.D., B. Tasic, K. Miyamichi, L. Li, and L. Luo. 2007. A global double-fluorescent Cre reporter mouse. *Genesis.* 45:593–605. http://dx .doi.org/10.1002/dvg.20335

Neufert, C., C. Becker, and M.F. Neurath. 2007. An inducible mouse model of colon carcinogenesis for the analysis of sporadic and inflammation-driven tumor progression. *Nat. Protoc.* 2:1998–2004. http://dx.doi.org /10.1038/nprot.2007.279

Normand, S., A. Delanoye-Crespin, A. Bressenot, L. Huot, T. Grandjean, L. Peyrin-Biroulet, Y. Lemoine, D. Hot, and M. Chamaillard. 2011. Nod-like receptor pyrin domain-containing protein 6 (NLRP6) controls epithelial self-renewal and colorectal carcinogenesis upon injury. *Proc.*

2250

IKKβ in intestinal mesenchymal cells promotes CAC | Koliaraki et al.

Natl. Acad. Sci. USA. 108:9601–9606. http://dx.doi.org/10.1073/pnas .1100981108

Pallangyo, C.K., P.K. Ziegler, and F.R. Greten. 2015. IKKβ acts as a tumor suppressor in cancer-associated fibroblasts during intestinal tumorigenesis. *J. Exp. Med*. 212:. http://dx.doi.org/10.1084/jem.20150576

Pasparakis, M., G. Courtois, M. Hafner, M. Schmidt-Supprian, A. Nenci, A. Toksoy, M. Krampert, M. Goebeler, R. Gillitzer, A. Israel, et al. 2002. TNF-mediated inflammatory skin disease in mice with epidermis-specific deletion of IKK2. *Nature*. 417:861–866. http://dx.doi.org/10 .1038/nature00820

Popivanova, B.K., K. Kitamura, Y. Wu, T. Kondo, T. Kagaya, S. Kaneko, M. Oshima, C. Fujii, and N. Mukaida. 2008. Blocking TNF-alpha in mice reduces colorectal carcinogenesis associated with chronic colitis. *J. Clin. Invest*. 118:560–570.

Schmidt-Supprian, M., W. Bloch, G. Courtois, K. Addicks, A. Israël, K. Rajewsky, and M. Pasparakis. 2000. NEMO/IKK gamma–deficient mice model incontinentia pigmenti. *Mol. Cell*. 5:981–992. http://dx.doi.org /10.1016/S1097-2765(00)80263-4

Servais, C., and N. Erez. 2013. From sentinel cells to inflammatory culprits: cancer-associated fibroblasts in tumour-related inflammation. *J. Pathol*. 229:198–207.

Shaker, A., M. Gargus, J. Fink, J. Binkley, I. Darwech, E. Swietlicki, M.S. Levin, and D.C. Rubin. 2014. Epimorphin(−/−) mice are protected, in part, from acute colitis via decreased interleukin 6 signaling. *Transl. Res.* 164:70–83. http://dx.doi.org/10.1016/j.trsl.2014.03.007

Terzić, J., S. Grivennikov, E. Karin, and M. Karin. 2010. Inflammation and colon cancer. *Gastroenterology*. 138:2101–2114.e5. http://dx.doi.org/10 .1053/j.gastro.2010.01.058

Trimboli, A.J., C.Z. Cantemir-Stone, F. Li, J.A. Wallace, A. Merchant, N. Creasap, J.C. Thompson, E. Caserta, H. Wang, J.L. Chong, et al. 2009. Pten in stromal fibroblasts suppresses mammary epithelial tumours. *Nature*. 461:1084–1091. http://dx.doi.org/10.1038/nature08486

Vandoros, G.P., P.A. Konstantinopoulos, G. Sotiropoulou-Bonikou, A. Kominea, G.I. Papachristou, M.V. Karamouzis, M. Gkermpesi, I.Varakis, and A.G. Papavassiliou. 2006. PPAR-gamma is expressed and NF-κB pathway is activated and correlates positively with COX-2 expression in stromal myofibroblasts surrounding colon adenocarcinomas. *J. Cancer Res. Clin. Oncol*. 132:76–84. http://dx.doi.org/10.1007/s00432-005 -0042-z

Wirtz, S., C. Neufert, B. Weigmann, and M.F. Neurath. 2007. Chemically induced mouse models of intestinal inflammation. *Nat. Protoc*. 2:541– 546. http://dx.doi.org/10.1038/nprot.2007.41

Yu, H., D. Pardoll, and R. Jove. 2009. STATs in cancer inflammation and immunity: a leading role for STAT3. *Nat. Rev. Cancer*. 9:798–809. http:// dx.doi.org/10.1038/nrc2734